 

ACOUSTICAL LETTER

# Application of Bergeron method for instantaneous longitudinal vibration analysis

Kenji Takahashi[1,*], Tomoatsu Ino[2] and Toru Yamazaki[2,†]

[1]*Graduate School of Kanagawa University, 3–27–1 Rokkakubashi, Kanagawa-ku, Yokohama, 221–0802 Japan*
[2]*Kanagawa University, 3–27–1 Rokkakubashi, Kanagawa-ku, Yokohama, 221–0802 Japan*

(*Received 28 January 2013, Accepted for publication 21 April 2013*)

**Keywords:** Bergeron method, Longitudinal vibration, Wave, Attenuation
**PACS number:** 43.40.+s [doi:10.1250/ast.34.361]

## 1. Introduction

The calculation of structural vibration by computational analysis methods such as finite-element analysis, the finite-difference method, and finite-difference time-domain method is extremely time-consuming. The Bergeron method [1–3] is well known as a fast computational method, and it has been applied in electromagnetism and acoustics [4]. However, there have been no reports on its application in the analysis of structural vibration. Therefore, we have developed a new extension of the Bergeron method for analyzing longitudinal vibration in a rod.

## 2. Bergeron method for longitudinal vibration in a rod

The theory behind the Bergeron method is described in detail in [1]. Here, we introduce a new formulation and procedure of the Bergeron method for the calculation of longitudinal vibration in a rod as an extension of the formulation for problems in electromagnetism shown in [2].

### 2.1. Analogy between structural and electric fields

The Bergeron method is based on the transmission line equation. The mobility analogy and the boundary continuity allow us to replace voltage and current with longitudinal velocity and axial stress, respectively.

### 2.2. Transmission line model

Consider a rod along the $x$ axis. The wave equation for longitudinal vibration in a rod is

$$\frac{\partial s(x,t)}{\partial x} = \rho \frac{\partial^2 \xi(x,t)}{\partial t^2}, \tag{1}$$

where $s$, $\xi$ are the axial stress and the longitudinal displacement and $\rho$ is the material density of the rod. The Voigt-Kelvin model is employed to express the axial stress $s$, which is expressed by

$$s = E\left\{\frac{\partial \xi(x,t)}{\partial x} + \varepsilon \frac{\partial}{\partial t}\left(\frac{\partial \xi(x,t)}{\partial x}\right)\right\}, \tag{2}$$

where $E$ is the Young's modulus of the rod and $\varepsilon$ is a loss factor. The transmission line equations in the frequency domain can be reduced to

$$\frac{\partial V(x,\omega)}{\partial x} = j\omega \frac{1}{AE(1+j\omega\varepsilon)} S(x,\omega) \tag{3a}$$

and

$$\frac{\partial S(x,\omega)}{\partial x} = j\omega A \rho V(x,\omega), \tag{3b}$$

where $V$ and $S$ are the Fourier spectra of the longitudinal velocity and axial force, respectively. The axial force $S$ is determined by the product of the axial stress $s$ and the cross-sectional area $A$ of the rod.

### 2.3. Node equation in frequency domain

Equations (3a) and (3b) are applied to derive the relationships between $V$ and $S$ at both ends of a transmission line with length $l$ (from $x = 0$ to $x = l$), as shown in Fig. 1.

The incident and reflected velocities at each end ($x = 0$ and $l$) are presented by $V^-(0,\omega)$, $V^+(0,\omega)$, and $V^-(l,\omega)$, $V^+(l,\omega)$, respectively. In this case, the node equations for the right end ($x = l$) of the line can be written by

$$V^+(l,\omega) = e^{-\gamma l} V^-(0,\omega), \tag{4a}$$

$$S(l,\omega) = -Z_s(\omega)\{V(l,\omega) - 2V^+(l,\omega)\}, \tag{4b}$$

and

$$V^-(l,\omega) = V(l,\omega) - V^+(l,\omega). \tag{4c}$$

Here, $Z_s(\omega)$ is the structural surge impedance, which is expressed by

$$Z_s(\omega) = -A\sqrt{\rho E(1+j\omega\varepsilon)}. \tag{5}$$

In an electric field, the wave propagation constant $e^{-\gamma l}$ is written as

$$e^{-\gamma l} = e^{-\alpha(\omega)\cdot l - j\omega\tau} = A(\omega)e^{-j\omega\tau}. \tag{6}$$

Here, $\alpha(\omega)$ is the attenuation constant, $\tau$ is the constant phase delay, and $A(\omega)$ is the attenuation characteristic of the line. On the other hand, since the phase delay in longitudinal vibration depends on the angular frequency, we consider a constant phase delay $\tau_0$ at an arbitrary angular frequency $\omega_0$ with a correction term $\Delta\tau$ which is written as

$$\tau(\omega) = \tau_0 + \Delta\tau(\omega). \tag{7}$$

Therefore, the wave propagation constant in longitudinal vibration can be expressed by

$$e^{-\gamma l} = A(\omega)e^{-j\omega\{\tau_0 + \Delta\tau(\omega)\}} \equiv A'(\omega)e^{-j\omega\tau_0}, \tag{8a}$$

and

$$A'(\omega) = e^{-\omega\alpha(\omega)\cdot l} e^{-j\omega\Delta\tau(\omega)}, \tag{8b}$$

where $A'(\omega)$ is the frequency-dependent attenuation characteristic. Equations (6) and (8a) are similar, and we can solve the

*e-mail: kenji_mypace@yahoo.co.jp
†e-mail: toru@kanagawa-u.ac.jp

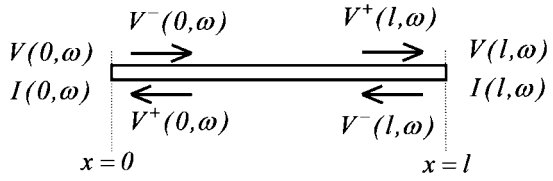


**Fig. 1** Transmission line with length $l$.

expressions for longitudinal vibration as well as that for the electric field. The relevant constants can be expressed by

$$\tau_0 = l\sqrt{\frac{\rho}{E\sqrt{1+\omega_0^2\varepsilon^2}}}\cos\frac{\varphi_0}{2} \tag{9a}$$

$$\varphi_0 = \tan^{-1}\omega_0\varepsilon \tag{9b}$$

and

$$\Delta\tau(\omega) = l\left\{\sqrt{\frac{\rho}{E\sqrt{1+\omega^2\varepsilon^2}}}\cos\frac{\varphi}{2} - \sqrt{\frac{\rho}{E\sqrt{1+\omega_0^2\varepsilon^2}}}\cos\frac{\varphi_0}{2}\right\} \tag{10}$$

2.4. Node equation in time domain

Equations (4a), (4b), and (4c) can be rewritten as follows in the time domain by performing inverse Fourier transform:

$$v^+(l,t) = a(t) * v^-(0,t-\tau), \tag{11a}$$

$$s(l,t) = -z_s(t) * \{v(l,t) - 2v^+(l,t)\} \tag{11b}$$

and

$$v^-(l,t) = v(l,t) - v^+(l,t), \tag{11c}$$

where $*$ denotes a convolution integral and $a(t)$ is the inverse Fourier transform of the wave propagation constant spectrum. Note that the node equation at the origin ($x = 0$) can also be expressed by using the above equations.

2.5. Procedure of calculation [2]

In order to evaluate the surge impedance $Z_s(\omega)$ and the attenuation characteristic $A'(\omega)$, we use modal approximations expressed by

$$Z_s(s) = z_c + \sum_i \frac{k_{y1i}}{1+sT_{y1i}} + \sum_j \frac{k_{y2j}\varsigma_{y2j}\omega_{y2j}s}{s^2+\varsigma_{y2j}\omega_{y2j}s+\omega_{y2j}^2}, \tag{12}$$

and

$$A'(s) = a_c + \sum_i \frac{k_{a1i}}{1+sT_{a1i}} + \sum_j \frac{k_{a2j}\varsigma_{a2j}\omega_{a2j}s}{s^2+\varsigma_{a2j}\omega_{a2j}s+\omega_{a2j}^2}, \tag{13}$$

where $s$ denotes the Laplace operator, $z_c$ and $a_c$ are the correction terms introduced in order to eliminate the inevitable steady-state error caused by a modal approximation by a finite number of modes. $T$, $k$, $\zeta$ and $\omega$ are the coefficients for each modal term.

The time response is calculated by solving recursive convolution equations of the second order, which are represented by

$$x_n = \alpha x_{n-1} + \lambda_1 u_n + \lambda_2 u_{n-1} \tag{14}$$

and

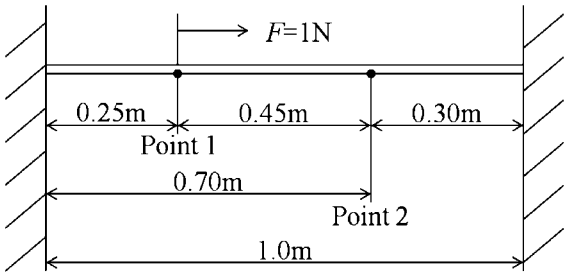


**Fig. 2** Test rod system.

$$y_n = \beta_1 y_n + \beta_2 y_{n-1} + \mu_1 u_n + \mu_2 u_{n-1} + \mu_3 u_{n-2}. \tag{15}$$

Here, $u$ is the input, $x$ and $y$ are the responses, the subscript $n$ indicates the time step, and $\alpha$, $\lambda$, $\beta$ and $\mu$ are the constants evaluated in the convolution integral.

## 3. Numerical simulation

Numerical calculation is carried out to verify the developed Bergeron method. The time response results are compared with those obtained by FEM.

3.1. Test system

A test model consisting of a simply supported steel rod with a cross-sectional area of $7.9 \times 10^{-5}\,\mathrm{m}^2$ and a length of 1 m is shown in Fig. 2. Young's modulus of the rod is 200 GPa, and its mass density is $7{,}834\,\mathrm{kg/m}^3$. The excitation force in the form of a Gaussian pulse with a maximum of 1 N is input at point 1 located at $x = 0.25$ m. The velocity responses of points 1 and 2 at $x = 0.7$ m are calculated, and the results are shown in Fig. 3.

In the calculation based on the developed Bergeron method, we consider three transmission line models with lengths of 0.25 m, 0.45 m, and 0.30 m because of the edges and the two responses. In the FEM calculation, we consider 1,000 finite elements with 1,001 nodes. The mass and stiffness matrices are built, and the damping matrix is obtained by taking the product of the stiffness matrix and the loss factor $\varepsilon = 10^{-6}$ based on the Voigt-Kelvin model. The displacement and velocity at each node are calculated by using the Runge-Kutta method.

3.2. Calculation results and discussions

Figure 3 shows a comparison of the complex attenuation characteristic $A'(\omega)$ calculated by FEM and the approximation in Eq. (13) based on the proposed method. The results are in good agreement, with a difference of less than 10%.

Figure 4 presents the velocity responses at points 1 and 2 calculated with the proposed method compared with the results calculated by FEM. These results are also in good agreement. Figure 4(a) shows the directly input incident wave and the wave reflected from the left end at $x = 0$ around $1.0 \times 10^{-4}$ s. Figure 4(b) shows the wave propagated from the excitation point around $1.0 \times 10^{-4}$ s and the reflected wave from $2.0 \times 10^{-4}$ s.

Thus, we verified the proposed formulation and calculation procedure of the Bergeron method for longitudinal vibration. Note that the computation time of the proposed method is less than 1/60 of the time required by FEM.

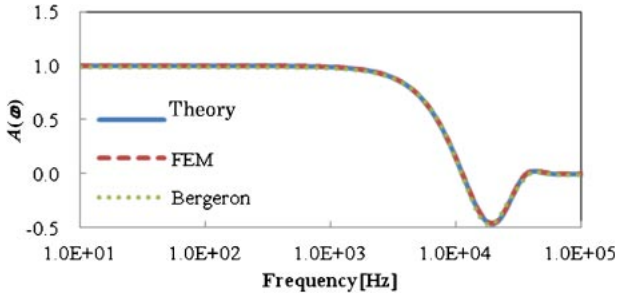


(a) Real part.

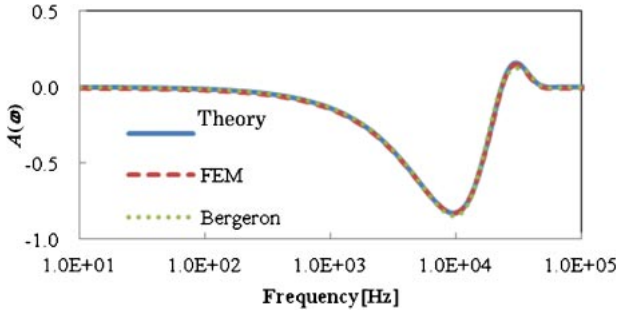


(b) Imaginary part.

**Fig. 3** Comparison of attenuation characteristic $A'(\omega)$ calculated by the Bergeron and finite element methods.

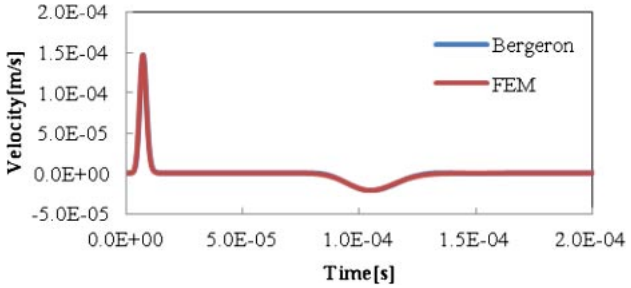


(a) Point 1.

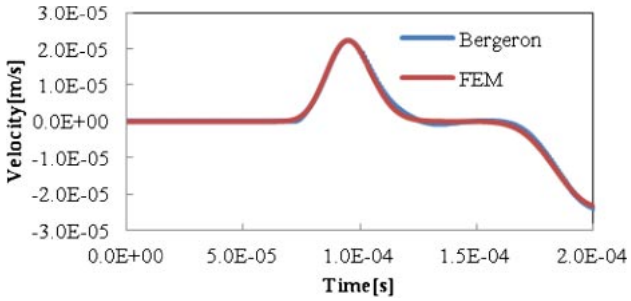


(b) Point 2.

**Fig. 4** Comparison of the velocity responses in time at two points along the $x$ axis.

## 4. Conclusion

We extended the Bergeron method for analyzing longitudinal vibration in a rod. The mobility analog and the boundary continuity allowed us to formulate the transmission line equations. The most important variables in the proposed method are the attenuation characteristic and the phase delay. The structural phase delay depends on the frequency and is expressed by a constant with an added correction factor. Numerical calculation of the longitudinal vibration was carried out to verify the proposed formulation and calculation procedure, and the results obtained with the proposed Bergeron method were in good agreement with those obtained by FEM. In future work, a further extension of the Bergeron method for flexural vibration of a beam will be introduced.

## References

[1] H. W. Dommel, "Digital computer solution of electromagnetic transients in single- and multiphase networks," *IEEE Trans. Power Appar. Syst.*, **PAS-88**, 388–399 (1969).

[2] T. Ino, "An approach for accurate modelling of frequency dependent effects of a double circuit DC transmission line on common tower," *Trans. IEEE Jpn.*, **110-B**, 395–403 (1990) (in Japanese).

[3] E. Qiang and Y. Xuechang, "Grounding insulation fault monitoring of power transformers using Bergeron's method," *Proc. IEEE TENCON '02*, pp. 1865–1868 (2002).

[4] K. Otabe, K. Kido *et al.*, "Simulation of transient wave propagation in sound absorbing material using Bergeron method," *Tech. Rep. IEICE*, EA98-125 (1999) (in Japanese).